Estuarine dissolved speciation and partitioning of trace metals: a novel approach to study biogeochemical processes

M. Abdou, M.-L. Tercier-Waeber, L. Dutruch, C. Bossy, F. Pougnet, A. Coynel, E. Bakker, G. Blanc, J. Schäfer

Estuarine dissolved speciation and partitioning of trace metals: a novel approach to study biogeochemical processes

Abdou M.[a*1], Tercier-Waeber M.-L.[a*], Dutruch L.[b], Bossy C.[b], Pougnet F.[b], Coynel A.[b], Bakker E.[a], Blanc G.[b], Schäfer J.[b]

[a]University of Geneva, Sciences II, 30 Quai E.-Ansermet, 1221 Geneva 4, Switzerland

[b]University of Bordeaux, Allée Geoffroy Saint-Hilaire, 33615 Pessac, France

Corresponding authors*: melina.abdou@ciimar.up.pt; marie-louise.tercier@unige.ch

Abstract

Estuaries are complex systems involving numerous biogeochemical gradients and processes that influence the behavior of trace metals. Lead (Pb), cadmium (Cd), and copper (Cu) speciation and partitioning were studied in the Gironde Estuary (SW France), using a multi-method approach in which data from innovative sensors and laboratory-based techniques were combined. For the first time in this system, the so-called dynamic fractions of the target metals (dissolved forms that are potentially bioavailable) were recorded on-board through voltammetry using unique antifouling gel-integrated microelectrode arrays (GIME) incorporated in a submersible sensing probe (TracMetal). Trace metals in the operationally defined dissolved < 0.2 µm and < 0.02 µm fractions, as well as complexed with suspended particles (collected after centrifugation) were quantified through sampling/laboratory-based techniques. High spatial resolution trace metal concentrations were monitored along the salinity gradient (S=0.10 to S=34.0) together with master bio-physicochemical parameters providing robust cruise-specific information on how well-known abiotic and biotic processes control the Gironde estuarine trace element partitioning, (i.e. conservative behavior, addition/removal). Combining conventional methods with GIME measurements showed: (i) the dominance of Cd dynamic species in the intra-estuarine total dissolved fraction (up to 90 %), (ii) the importance of small colloids as trace metal carrier phases, desorbing and complexing dynamic fractions of Pb and Cu, and (iii) the potential influence of photo-redox processes remobilizing Pb under their dynamic forms (up to 80 %). Data also suggest trace metal release/sorption by phytoplankton with an increase of dissolved Cu concentrations in

[1]Present address: CIIMAR, Avenida General Norton de Matos, S/N; 4450-208 Matosinhos, Portugal

the riverine branch, as well as Cu and Cd particulate concentrations showing higher levels towards productive coastal waters. This complete approach allowed to monitor key estuarine biogeochemical processes and highlighted the valuable use of the TracMetal to record subtle variations of potentially bioavailable dissolved metal fractions.

Keywords

Lead; Cadmium; Copper; Priority Substances; Potentially Bioavailable Dissolved Fraction; Suspended Particles

1. Introduction

Trace metals in aquatic systems are distributed as numerous chemical species, comprising free hydrated ions, their complexes with various inorganic and organic ligands and colloids (of 1 nm to 0.2 µm size) and other suspended particles of size > 0.2 µm (Tercier-Waeber et al., 2012). Transformations among the various metal species are usually reversible, with the important consequence that the speciation of a metal is a function of the bio-physicochemical conditions of the medium. Any variation of the speciation of a metal will influence its transport, reactivity and potential ecotoxicological impact. A comprehensive study of trace metal biogeochemical cycles must therefore include the determination of specific metal species or the group of homologous metal species (i.e. metal speciation). In addition, the partitioning between dissolved and particulate phases changes in response to the surrounding environment, particularly along estuarine gradients. The degree of metal sorption and desorption depends on the type of particulate matter present in the water column (Sanders and Abbe, 1987).

Most trace metals released into aquatic systems originate from land-based human activities and estuaries often represent recipient waters of riverine pollution at the whole watershed scale (Tercier Waeber et al., 2015). Estuaries are complex systems where the mixing of fresh- and seawaters from the upper tidal zone to the outer estuary generate gradients of salinity and turbidity. These systems undergo major biogeochemical transformations that influence the export of contaminants to the ocean (e.g. Larrose et al., 2010). The Gironde Estuary is a major European estuary considered as a model for physical, hydrological, and geochemical studies, and especially for estuarine trace element transport and reactivity. Intense past and present agricultural activity, wastewater discharge and historical metal pollution originating from former industrial/metallurgic activities in

its watershed have strongly affected the environmental quality of the estuary and the adjacent coast (Coynel et al., 2009; Deycard et al., 2017; Larrose et al., 2010; Masson et al., 2006; Petit et al., 2013; Schäfer et al., 2002; Strady et al., 2011). Trace metal contamination and biogeochemical behavior along this fluvial-estuarine continuum have been thoroughly studied since decades (Audry et al., 2007; Elbaz-Poulichet et al., 1984; Kraepiel et al., 1997; Michel et al., 2000; Pougnet et al., 2021). However, a lack of knowledge still exists for various biogeochemical processes. This includes the importance of small colloids (< 0.02 µm) for trace metal distribution and transport, the bioavailability of trace metals in such complex systems, and the influence of primary producers on trace metal speciation, especially in the coastal productive zone. Indeed, the literature reports that effects of metals on phytoplankton are reciprocal and that biota and particularly phytoplankton may have profound effects on trace metal chemistry through sorption processes (Sunda, 1989). In particular, lead (Pb) and cadmium (Cd), identified as priority substances by European regulations, as well as copper (Cu) have, over the past decades, presented anomalously high concentrations in various tributaries within the Gironde Estuary watershed (Masson et al., 2006). These trace metals are considered essential and/or toxic for aquatic organisms that can bioaccumulate them and in turn alter their chemical forms (e.g. Sunda, 1989). We therefore require precise monitoring of these trace elements at high spatial resolution that allows for the accurate quantification of specific metal fractions, especially the potentially bioavailable dissolved forms. Voltammetric sensors represent promising tools for direct determination of metallic pollutants in the aqueous phase (e.g. Nezamzadeh-Ejhieh and Shahanshahi, 2013). In particular, recent analytical developments based on *in situ* or on-board electrochemical measurements of the so-called dynamic dissolved metal fractions using antifouling gel-integrated sensors allow for highly sensitive, reliable, and frequent data acquisition bringing new information for the monitoring and understanding of trace metal biogeochemical processes in marine systems (Penezić et al., 2020; Tercier-Waeber et al., 2021b, 2021a).

The objectives of the present work are therefore to perform the first assessment of the dynamic fraction of Pb, Cd, and Cu along the salinity gradient of the Gironde Estuary at high spatial resolution, and to use the data from the innovative sensing approach together with classical methodologies to better understand the biogeochemical behavior of trace metal species in terms of dissolved speciation and partitioning in this representative system.

2. Material and methods

2.1. Sampling area and strategy

The Gironde Estuary (~ 170 km length) is impacted by multi-metal pollution (including Cd, Cu, Zn, and Pb) which originates from a common point source that is a former mining and smelting industry and affects the fluvial-estuarine continuum since decades (Pougnet et al., 2021). This industry, located in Decazeville and active from 1842 to 1987, has led to metal concentration enrichment of the riverine system (Audry et al., 2004). The Gironde Estuary is formed from the meeting of the Garonne (its major tributary) and the Dordogne River (total watershed ~ 80,000 km^2; Figure 1). It hosts important urban sectors along its riverine areas, mainly the Garonne River with the Bordeaux conurbation (~ 1 million inhabitant equivalents; Deycard et al., 2014; "Insee.fr"). Hydrodynamic characteristics of the Gironde Estuary have been thoroughly described in the literature (e.g. Jalón-Rojas et al., 2015). This is a partially mixed to well-mixed estuary, characterized by a semi-diurnal meso- to macro-tidal regime and a maximum turbidity zone (MTZ) where concentrations of Suspended Particulate Matter (SPM) exceed 1 $g.L^{-1}$ in surface water. Water residence time was estimated to ~ 20 – 90 days for high and low water discharge periods, respectively, while estimated particle residence time is 1 – 2 years (Jouanneau et al., 1993). The field campaign was carried out in June 2017 (16^{th}-21^{st}) on board the R/V Thalia and consisted in a longitudinal profile along the estuarine salinity gradient (practical salinity "S"; S=0.10 to S=34.00; Figure 1) with four sampling sites in the Garonne River Branch (1-4), the following twelve down the Gironde Estuary (5-16), and four samples in the north channel of the outer estuary (17-20). Four samples were collected along the south channel of the outer estuary (21-24). Sampling was carried out during low river discharge conditions (Q ~ 235 $m^3.s^{-1}$; Garonne and Dordogne) and spring tide regime (tidal coefficient and range of 50 – 75 and 2.5 - 3.6 m, respectively).

2.2. Sample collection and analytical methods

Sampling. Subsurface water samples were collected with a pre-cleaned Niskin bottle at ~1m depth and transferred into acid-cleaned polypropylene (PP) bottles that were previously rinsed three times with subsurface water from the site. Suspended particles were retrieved using a peristaltic pump

with PP tubing and collected by centrifugation (12,000 g, Westfalia®; Schäfer and Blanc, 2002). Samples were collected during daytime, except for one sample at site 16, S=28 (Figures 1 and 2c).

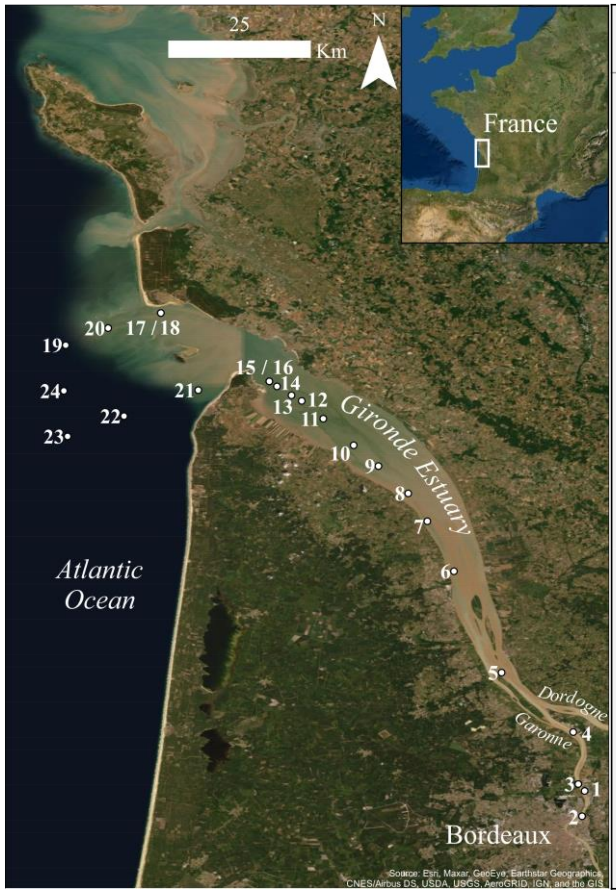

Site	Salinity	Site	Salinity
1	0.10	13	22.30
2	0.20	14	25.15
3	0.60	15	26.70
4	1.10	16	28.10
5	3.00	17	29.95
6	4.30	18	30.45
7	6.00	19	32.70
8	9.05	20	34.00
9	11.85	21	29.90
10	15.35	22	32.90
11	17.95	23	31.85
12	20.00	24	32.75

Figure 1: Map of the study area with sampling sites and corresponding salinity. Left: site locations along the salinity gradient (1 to 20) and the four coastal sites in the south channel (21 to 24); Right: the practical salinity (S) determined at each site.

".

Dynamic metal fraction (Me_{dyn}). Quantification of Me_{dyn} was performed by subtractive square wave stripping voltammetry (SWASV) on two gel-integrated microelectrode arrays (GIME) sensors implemented in the TracMetal sensing probe (channels 1 and 2). The GIME used in this application consisted of on-chip 190 interconnected iridium- (Ir)-based microdisk arrays of 5 µm in radius (Fighera et al., 2016), electroplated with mercury (Hg) micro-hemispheres and covered with an antifouling agarose gel (Buffle and Tercier-Waeber, 2005). A detailed description of the TracMetal, a three-channel submersible probe designed for simultaneous *in situ* measurements of

a range of (priority) hazardous trace metals using various GIME sensors, can be found elsewhere (Tercier-Waeber et al., 2021b). Because of time constraints related to the cruise trajectory, the TracMetal was not deployed *in situ*. The Me_{dyn} quantification was performed on-board applying the TracMetal after placing 1 L of sub-surface water sample freshly collected in an acid-cleaned PP bottle.

Sensors were calibrated before and after field monitoring in the on-board laboratory. Calibrations were performed in dinitrogen- (N_2)-purged sodium nitrate (0.1 M $NaNO_3$; Suprapur Merk®) solutions spiked with Cd(II), Pb(II), and Cu(II) in ranges of 0.1 to 0.6 $\mu g.L^{-1}$, 0.2 to 1.2 $\mu g.L^{-1}$ and 0.2 to 1 $\mu g.L^{-1}$, respectively. Individual stock solutions of Cu, Pb, and Cd used for the calibration were prepared by appropriate dilution of a 1 $g.L^{-1}$ atomic absorption standard solution (Aldrich®) in HNO_3 and acidified to pH 2 with HNO_3 (14 M Suprapur, Merck®). The subtractive SWASV protocol and conditions used were as follows: after a cleaning phase at 70 (S<10) or -50 mV (S>10) for 1 min, metals were pre-concentrated at – 1200 mV for a given time (typically 10 min for calibration; 20 min for on-board measurements). The potential was then scanned from - 1200 to – 50 or 70 mV (stripping step) with a pulse amplitude of 25 mV, a step amplitude of 8 mV, and a frequency of 200 Hz. After each measurement, a background scan was recorded, using the same parameters, but with shortened pre-concentration time (5 s). The background scan was subtracted from the analytical scan to obtain a corrected final scan (Tercier Waeber et al., 1998). Standard deviations of the calibration slopes obtained before and after field measurements were < 10 % for the three metals, demonstrating the excellent stability of the Hg hemispheres and the absence of fouling during the 6 days of on-board monitoring. The Me_{dyn} concentrations were determined from the temperature effect corrected subtractive SWASV signals (Tercier-Waeber et al., 1999) and the average values of the calibration slopes, both normalized by the pre-concentration time. The lower detection limits, calculated on the basis of 3.3 x the standard deviation of the regression lines divided by the slopes, were 0.7, 1 and 6.6 $ng.L^{-1}$ for Cd(II), Pb(II), and Cu(II), respectively. Vertical error bars in the graphics of the Me_{dyn} longitudinal profiles represent the maximum Relative Standard Deviation (RSD%) determined from the two replicate measurements performed with the two GIME in each sample (i.e. n = 4): 6 % for Cd(II) and 8 % for Pb(II) and Cu(II). The accuracy of the GIME was demonstrated by inter-comparison exercises performed by EU laboratories (Braungardt et al., 2009).

Dissolved 0.2 and 0.02 µm metal fraction ($Me_{0.2}$ and $Me_{0.02}$). Water samples were immediately filtered on-site through 0.2 µm cellulose acetate filters ($Me_{0.2}$; Minisart, Sartorius®) and through 0.02 µm alumina-based filters ($Me_{0.02}$; Whatman®). Filtrates were placed into acid-cleaned PP bottles and acidified with HNO_3 (1/1000 v/v; Ultrapure J.T. Baker ®, 14 M). Samples were then stored at 4 °C in the dark pending analysis. Field blanks using Milli-Q water were performed for all sampled parameters and processed in the same way as natural water samples. The $Me_{0.2}$ and $Me_{0.02}$ were quantified through Inductively Coupled Plasma-Tandem Mass Spectrometry (ICP-MS/MS; Thermo Scientific®; iCAP TQ) using Argon Gas Dilution (AGD) allowing direct analysis of estuarine waters without any prior dilution (Dutruch et al., 2019). Considering relatively important changes in the signal response according to sample salinity, dissolved concentrations were quantified using standard addition method adapted to three different salinity ranges (0.1 to 10, 10 to 30, > 30).

Analyses of Certified Reference Material (CRM) for estuarine waters (SLEW-3, NRC) provided recoveries of ~ 100 % for Mn and Fe, ~ 110 % for Cu and Cd and of ~ 130 % for Pb. Precision (RSD%) was of ~ 5 % for Mn, Fe, Cu and Pb and ~ 10 % for Cd (n = 5; vertical error bars in the graphics). Analyses of CRM for coastal waters (CASS-6, NRC) provided recoveries of ~ 80 % for Fe, ~ 90 % for Mn, ~ 110 % for Pb, Cd, and Cu and RSD% of 5 % for Mn, Fe, and Cu and ~ 15 % for Cd and Pb (n = 5; vertical error bars in the graphics). The longitudinal profile of Fe_{diss} and Mn_{diss} was previously presented in Penezić et al. (2020).

Particulate metal fraction (Me_{part}). The particulate samples obtained after centrifugation of suspended particles were dried (50 °C, 48 h), powdered and homogenized with an agate mortar. Samples were stored in sealed PP containers and kept in the dark at room temperature pending digestion and analysis. Representative subsamples (~ 30 mg) of particulate material, CRM and method blanks were acid digested. This step was performed in closed PP tubes (DigiTUBEs®, SCP SCIENCE) in a heating block (2 h at 110 ºC) using 1.5 mL hydrochloric acid (HCl; 10 M Suprapur, Merck®), 750 µL HNO_3 (14 M Suprapur, Merck®) and 2.5 mL hydrofluoric acid (HF; 29 M Suprapur, Fisher®), as described elsewhere (Gil-Díaz et al., 2018; Lerat-Hardy et al., 2021). After evaporation to dryness, we performed re-dissolution with 250 µL HNO_3 (14 M) at 110 °C and, after cooling, the samples were brought to 10 mL using Milli-Q water. The Me_{part} were quantified by ICP-MS (XSeries 2, Thermo Scientific®) applying external calibration. Stream and estuarine sediments CRM (NCS DC 73307 and BCR®-277R, respectively) were analyzed for quality

control. They provided recoveries > 90% and precision of ~ 5 % (n = 3; vertical error bars in the graphics).

Ancillary measurements. Particulate Organic Carbon (POC) concentrations in surface water were determined by filtration of precise water volumes through pre-combusted and pre-weighed filters (Whatman® GF/F, 0.7 µm). The filters were rinsed with MilliQ water to remove salts and were then oven dried to constant weight at 50 °C and weighed again. The weight difference provided the SPM concentrations. Filters were then kept in the dark at room temperature pending analysis. They were analyzed with a LECO© CS-125 after carbonate elimination with 2M HCl as described elsewhere (Etcheber et al., 2007). Analytical quality was checked by measuring CRMs (e.g. LECO 501–503) providing recovery of ~ 95 %. Physical-chemical parameters including practical salinity (S), temperature, oxygen saturation level (O_2 sat), and pH were measured in collected samples with portable TetraCon 325 and Sentix 41 probes (PROFILINE®, WTW). Finally, we retrieved information on solar radiation from "Meteo France", tidal information from the website "maree.info", and river discharges from the National Hydrographic Agencies (Banque Hydro database).

2.3. Data treatment

Normalization of particulate metal concentration. It is essential to consider lithogenic trace metal variability before evaluating the influence of anthropogenic inputs (Loring and Rantala, 1992). Also, in most aquatic systems, hydro-sedimentary processes fractionate particles according to parameters such a grain size, density and shape inducing mineralogical (chemical) bias due to the common observation that trace metal concentrations tend to increase with decreasing sediment grain sizes. Thorium (Th), which must be lithogenically controlled (Marmolejo-Rodríguez et al., 2008) and which does not originate from any anthropogenic inputs in our study area, served as a proxy to normalize variations from lithogenic sources. It is also useful to correct potential variations due to grain size effects as already applied in previous studies in the Gironde fluvial–estuarine system (e.g. Coynel et al., 2007; Larrose et al., 2010).

Partitioning. Trace metal particle/water distribution coefficients i.e. partition ratio, P, were calculated following the Eq 1 (McKinley and Alexander, 1992):

$$P = Me_{part} / Me_{0.2} \quad \text{(Eq1)}$$

220 Values are shown in Supporting Information (Figure S1).

221 ***Proportion of the dissolved metal fractions.*** Three specific homologous metal fractions were
222 defined, based on their size and complex lability, as follows: (1) The Me_{dyn} obtained by direct
223 GIME-SWASV measurements. This fraction includes the free metal ions and the small sufficiently
224 mobile (size $\leq$ 4 nm) and labile (fast dissociation rates) metal complexes that are potentially
225 bioavailable (Buffle and Tercier-Waeber, 2005). (2) The small colloidal metal species ($Me_{col<0.02}$)
226 obtained by subtracting Me_{dyn} from $Me_{0.02}$ and including the metals adsorbed on small inorganic
227 colloids or forming inert complexes with organic ligands. (3) The inorganic and organic colloidal
228 metal species ($Me_{0.02<col<0.2}$) obtained by subtracting $Me_{0.02}$ from $Me_{0.2}$. Graphical representation of
229 the different fractions using interpolations were performed with IGOR PRO (WaveMetrics®;
230 Figure S2).

231 ***Effective solar radiation.*** Variations of solar radiation intensity on the water column may induce
232 various changes of trace metal speciation through photochemical reactions (e.g. photolysis of
233 dissolved organic matter, photo-induced reduction/oxidation of inorganic colloids) and/or biotic
234 sorption (e.g. following phytoplankton development). Yet, ambient SPM concentrations found in
235 the estuarine gradient may limit both processes. Normalization of instantaneous solar radiation by
236 SPM concentration (rad/SPM) should account for light attenuation by SPM and thus be related
237 with the effective light abundance available for photo-redox mechanisms (Castelle et al., 2009).
238 Correlations of the different trace metal fractions with rad/SPM (except for sites 21-24 with
239 relatively very low SPM < 15 $mg.L^{-1}$) are given in Table S1.
240

3. Results

3.1. Hydrological conditions and ancillary parameters

Salinity ranged from 0.10 to 34.0 (Figure 1). Temperature as well as pH values followed the salinity gradient with increasing pH and decreasing temperatures from the freshwater endmember towards the coastal Atlantic Ocean (7.62 to 8.19, 25.1°C to 19.0°C, respectively; Figure 2a). After maximum SPM values of 1,600 $mg.L^{-1}$ (Figure 2b), decreasing SPM trend was observed for low salinities with values reaching 91.35 $mg.L^{-1}$ at S=4.3. Thereafter, SPM levels showed a slight increase between S=5 and S=15 followed by rather constant values in the mid-estuary (123 ± 6 $mg.L^{-1}$). Estuary mouth concentrations were slightly lower (63 ± 7 $mg.L^{-1}$) and a peak value (~ 1000 $mg.L^{-1}$) was observed at S=28.1. Coastal SPM concentrations were drastically lower at 8 ± 1 $mg.L^{-1}$ in the south channel. The oxygen saturation levels (O_2 sat) displayed first a decrease from 96.1 % at S=0.1 to ~ 80 % at S=0.2 and S=0.6 (Figure 2c). An increasing trend followed this pattern, with values over 100 % in the estuary mouth. Particulate Organic Carbon/SPM ratio (POC%) showed a decreasing trend in the riverine branch going from ~ 2 % to 1 % (Figure 2d) and an increasing pattern along the salinity gradient with relatively high values of 15 % reached at external sites. After a decreasing trend in the riverine branch ($Fe_{0.2}$ from 0.86 to 0.61 $\mu g.L^{-1}$; $Fe_{0.02}$ from 0.82 to 0.51 $\mu g.L^{-1}$), $Fe_{0.2}$ varied from 0.75 to 1.3 $\mu g.L^{-1}$, and from 0.49 to 0.69 $\mu g.L^{-1}$ for $Fe_{0.02}$, showing an increasing trend seaward (Figure 2e). The $Mn_{0.2}$ and $Mn_{0.02}$ were very similar and ranged between ~ 0.07 and 7 $\mu g.L^{-1}$ with a clear increasing trend along the salinity gradient (Figure 2f).

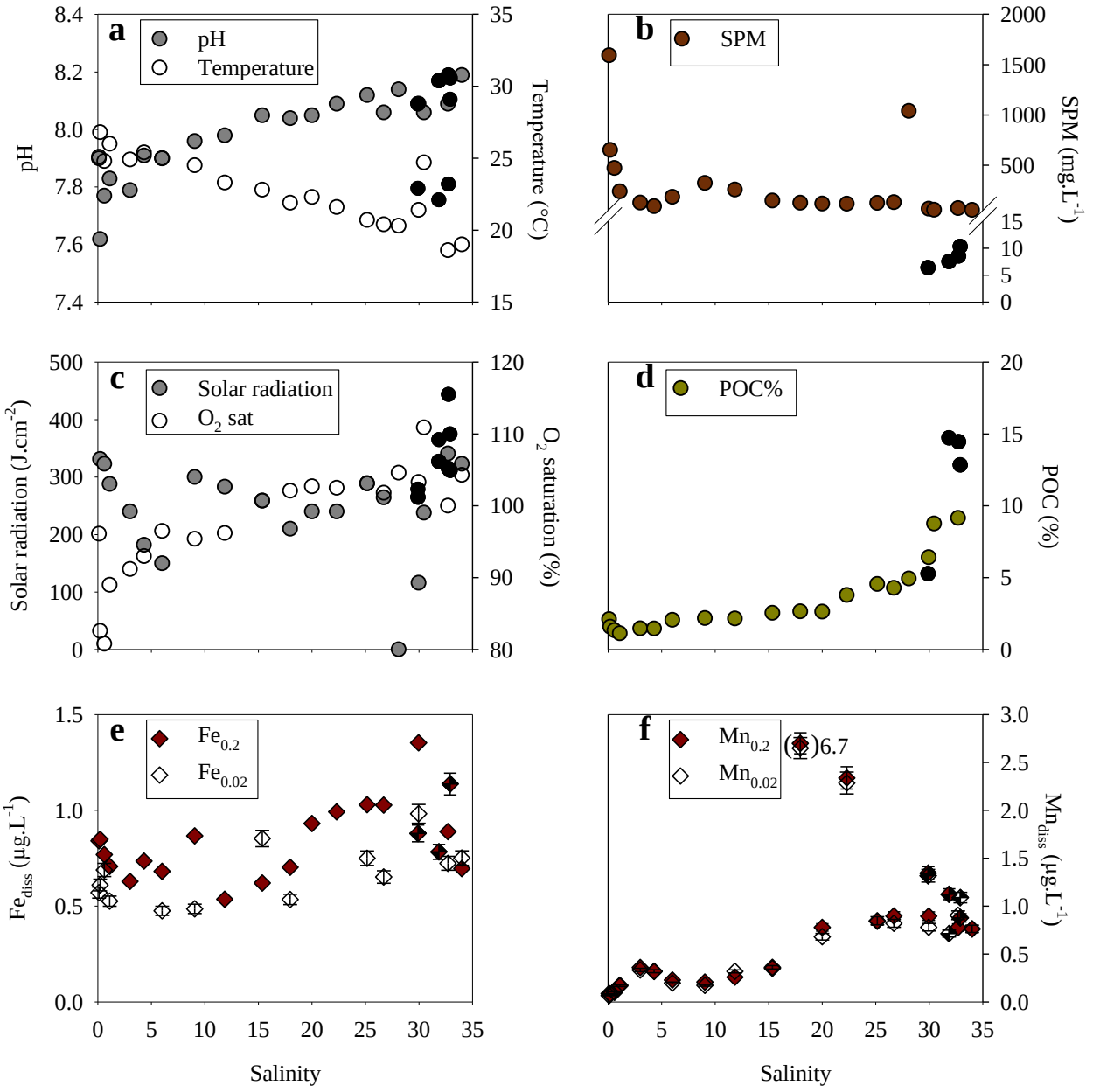

Figure 2: Longitudinal profiles of major physical-chemical parameters and dissolved Fe and Mn concentrations. a: pH and temperature; b: Suspended Particulate Matter (SPM); c: solar radiation and oxygen saturation level (O_2 sat); d: Particulate Organic Carbon / SPM ratio (POC%); dissolved concentrations in 0.2 and 0.02 fractions of Fe and Mn (e, f; Penezić et al., 2020). Half-black symbols correspond to coastal sites in the south channel. Values out of the range (presumed outliers) are presented in parentheses.

3.2. Trace metal longitudinal profiles

Lead

In the fluvial estuary (S=0.1 to S=1.1), a decreasing trend was observed for $Pb_{0.2}$ and $Pb_{0.02}$ (0.04-0.03 µg.L^{-1} respectively, to 0.02 µg.L^{-1}; Figure 3a). Along the estuary, the slightly decreasing trend in $Pb_{0.02}$ continued, reaching a minimum of 0.006 µg.L^{-1} at S=32.7. In contrast, $Pb_{0.2}$ did not show a well-defined spatial trend, with highest values for salinities ranging from S=22.3 to S=28.1 and slightly lower concentrations in the lower estuary compared to the upper estuary. In the coastal waters, the concentrations were similar to those in the lower estuary for $Pb_{0.2}$ (0.016 to 0.022 µg.L^{-1}) and slightly higher for $Pb_{0.02}$ (0.011 to 0.017 µg.L^{-1}). The Pb_{dyn} showed a slightly decreasing trend from 0.002 to 0.001 µg.L^{-1} in the riverine part of the estuary and then a linear increase (0.002 to 0.005 µg.L^{-1}; Pearson r = 0.83) along the salinity gradient (Figure 3a). Two small Pb_{dyn} peaks were observed first from S=9 to S=15, then from S=22 to S=28. The four southern coastal sites displayed higher Pb_{dyn} (0.012 to 0.014 µg.L^{-1}) reaching concentration levels similar to $Pb_{0.02}$.

The Pb_{part} suggested a decreasing trend in the Garonne Branch (S≤1.1; from 64 to 41 mg.kg^{-1}) as well as in the lower estuary (S≥27; from 83 to 56 mg.kg^{-1}) and southern coastal sites (from 71 to 44 mg.kg^{-1}), while a rather constant value close to 60 mg.kg^{-1} was observed for 3 <S<27 (Figure 3b).

Cadmium

The concentrations of the different Cd fractions measured in the water column are reported in Figure 3c showing similar $Cd_{0.2}$ and $Cd_{0.02}$ concentrations. From S=0.10 to S=17.95 i.e. to the mid-estuary (site 11, Figure 1) concentrations increased from 0.01 to 0.07 µg.L^{-1} then decreased towards coastal waters, reaching again concentrations of ~ 0.01 µg.L^{-1}. The Cd_{dyn} ranged from 0.003 to 0.007 µg.L^{-1} in the fluvial estuary (S≤1.1), increased up to 0.07 µg.L^{-1} at S≤22.3, then decreased to 0.009 µg.L^{-1} near the estuary mouth.

The Cd_{part} showed two similar decreasing trends from ~ 0.50 to 0.35 mg.kg^{-1} both in the riverine branch (S=0.1 to S=0.6) and along the estuarine gradient (S=3 to S=32.7). The four southern coastal sites displayed an increasing trend with Pb_{part} varying from 0.42 to 0.94 (S=29.9 to S=32.75).

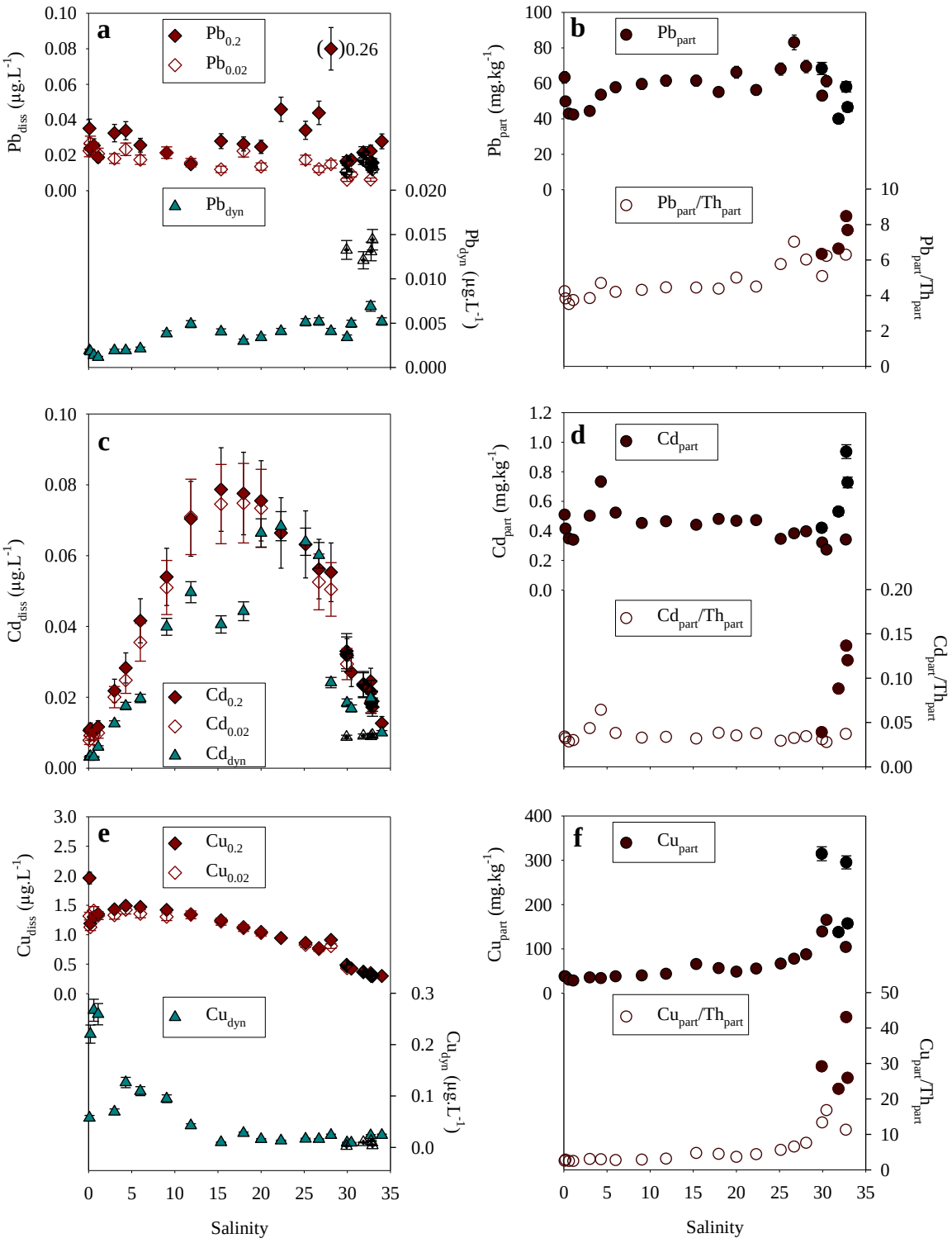

Figure 3: Longitudinal profiles of trace metal concentrations in the different dissolved and particulate fractions. Metal dissolved 0.2 µm ($Me_{0.2}$), 0.02 µm ($Me_{0.02}$), and dynamic (Me_{dyn}) fractions for Pb, Cd, and Cu (a, c, and e, respectively, $\mu g.L^{-1}$); metal particulate concentrations (Me_{part}, $mg.kg^{-1}$) and Th-normalized Me_{part} (Me_{part}/Th_{part}) for Pb, Cd, and Cu (b, d, and f, respectively). Half-black symbols correspond to coastal sites in the south channel. Values out of the range are presented in parentheses.

Copper

Both $Cu_{0.2}$ and $Cu_{0.02}$ showed similar concentrations and spatial trends (Figure 3e). Maxima were recorded at S=0.1 with $Cu_{0.2}$ and $Cu_{0.02}$ of 2.0 and 1.3 $\mu g.L^{-1}$, respectively. Then in the upper estuary, a slight increase in both, $Cu_{0.2}$ and $Cu_{0.02}$ occurred from 1.2 to 1.5 $\mu g.L^{-1}$ and 1.1 to 1.4 $\mu g.L^{-1}$, respectively (S=0.2 to S=4.3). This is followed by a subsequent seaward decrease down to ~ 0.3 $\mu g.L^{-1}$ for both fractions. The $Cu_{dyn,}$ represented a minor proportion and showed a different profile with highest values in the riverine part, reaching 0.27 $\mu g.L^{-1}$ and thereafter decreasing to a minimal, constant value of ~ 0.01 $\mu g.L^{-1}$ from S=15 to the outer estuary (Figure 3e).

The Cu_{part} showed a decreasing trend for S=0.1 to S=1.1 with values varying from 40 to 30 $mg.kg^{-1}$ (Figure 3f). This is followed by an increasing trend with southern coastal values of up to 315 $mg.kg^{-1}$.

4. Discussion

4.1. Behavior of trace metal species

Lead

The similar $Pb_{0.2}$ and $Pb_{0.02}$ coupled to the lower Pb_{dyn} along the longitudinal profile suggests that colloids in the size range 0.2-0.02 µm are negligible or have only a minor influence on Pb_{diss} variations. On the other hand, small colloids (< 0.02 µm) may play an important role in the transport and fate of Pb and especially on the proportion of its potentially bioavailable fraction.

Estuarine Pb reactivity includes rapid adsorption onto suspended particles, influencing Pb_{diss} removal (Chiffoleau et al., 1994). The interaction energy between colloids and associated trace metals results essentially from long range electrostatic interactions and short range attractive van der Waals forces that are predominant in marine and estuarine waters owing to increasing ionic strength (Tercier-Waeber et al., 2012). An increasing fraction of colloidal trace metals, organic matter (OM), and dissolved organic metal complexes is therefore expected throughout the salinity gradient (Seijo et al., 2009), while colloid aggregation is also promoted (Elbaz-Poulichet et al., 1984; Tercier Waeber et al., 2012). Colloid coagulation may therefore partly explain Pb_{diss} removal with increasing salinity along the riverine branch. In addition, increase of Pb_{dyn} along the salinity gradient may reflect a Pb mobilization towards its potentially bioavailable form. The opposite trend observed between Pb_{dyn} and $Pb_{0.02}$ suggests Pb desorption from small colloids throughout the salinity gradient and subsequent gradual increase of its dynamic forms (Figure S2a).

In the southern coastal sites, the observed $Pb_{0.02}$ displayed some values lower than Pb_{dyn}, suggesting a potential analytical bias and an under-estimation of $Pb_{0.02}$. A preconcentration of colloids and/or OM at the membrane surface by promoting Pb adsorption/complexation could explain this bias, as this would decrease Pb in the dissolved phase. The nature of colloids in the coastal zone might differ from the one along the estuary, with a likely dominance of organic colloids complexing dissolved Pb. Indeed, literature reports that a non-negligible part of Pb is complexed with organic ligands (e.g. Elbaz-Poulichet et al., 1984). This assumption is also supported by the longitudinal profile of Pb_{part}. Accordingly, while the Pb_{part} decrease for low salinities was associated to lithogenic effects (with only a slight decrease of Th-normalized Pb_{part}), the normalized-Pb_{part} showed an increasing trend from S > 25 up to the estuary mouth (Figure 3b), along with a parallel

POC increase from 5 to 15 % (Figure 2d). This pattern might reflect Pb adsorption on POC and suggest an organic origin of Pb ligation that could possibly be biogenic (algal cell debris and/or their exudates; e.g. Illuminati et al., 2019). Previous studies on Pb_{part} speciation through sequential extractions have shown that the carbonate-bound and exchangeable Pb_{part} decreased over the salinity gradient while bound Fe-Mn oxides and organic Pb_{part} increased (Elbaz-Poulichet et al., 1984), supporting our observations. Similar Pb_{part} concentration levels and longitudinal trend were recorded in 1982 and 1994 studies (Elbaz-Poulichet et al., 1984; Kraepiel et al., 1997). Following this hypothesis, maximum Pb_{dyn} recorded outside the estuary may correspond to Pb release due to photoreduction/oxidation of inorganic/organic ligands. In fact, Pb remobilization from Pb-bearing complexes (Elbaz-Poulichet et al., 1984; Pinedo-Gonzalez et al., 2014) and a subsequent increase of Pb_{dyn} in the water column may occur in coastal waters with very low SPM and significant solar radiation. Such processes might also contribute to the two relatively high Pb_{dyn} values along the gradient (S~12 and 25) that occurred at peaks of solar irradiation (Figures 2c and 3a) as further discussed in *Section 4.2*.

Overall, the slight decreasing trend characterizing $Pb_{0.2}$ and $Pb_{0.02}$ along the salinity gradient suggests that the estuary is a source of Pb_{diss} to the coastal waters. Previous studies on Pb_{diss} variations in this system confirmed a general decrease of the concentrations from the river endmember to the sea (< 0.45 µm; Elbaz-Poulichet et al., 1984; Kraepiel et al., 1997). However, reported Pb_{diss} levels of the Gironde Estuary were about 10 to 20 times higher in 1982 (Elbaz-Poulichet et al., 1984) than the present data, while the concentrations at low salinity were about twice higher in 1994 (Kraepiel et al., 1997). This suggests a decrease of anthropogenic inputs of Pb_{diss} to the system over time as observed for Cd (Pougnet et al., 2021) with the remediation works in the Decazeville watershed and potentially the elimination of Pb in gasoline (e.g. Boyle et al., 2014). This is in line with ongoing resilience of the historical metal contamination in the watershed (Schäfer et al., 2021).

Cadmium

The spatial variation of the $Cd_{0.2}$ and $Cd_{0.02}$ fractions showed the typical "bell-shape" trend observed also earlier for dissolved Cd in the Gironde Estuary (e.g. Dabrin et al., 2009; Pougnet et al., 2021) as well as in other estuarine environments, e.g. the Mississippi (USA; Shiller and Boyle, 1991) and the Seine Estuary (France; Chiffoleau et al., 1994). The non-conservative behavior (addition) observed from S=0.1 to mid-salinity range (S=15-20) is explained by an efficient Cd remobilization from the particulate phase due to increasing chloride-complexation (Bourg, 1987; Waeles et al., 2005) implying a strong decrease in the partition coefficient P_{Cd} (Figure S2c). From the mid-salinity range towards the sea, dilution by Cd-poor oceanic water becomes dominant due to the absence of important net mobilization from particles to the dissolved phase (e.g. Dabrin et al., 2009). The fact that $Cd_{0.2}$ and $Cd_{0.02}$ are almost identical all over the salinity gradient clearly indicates that coarse colloids (>0.02 µm) play a minor role in dissolved Cd speciation. The Cd_{dyn} variations also mainly displayed a bell-shape with similar concentrations than other Cd_{diss} and represented up to 80 % for S=22.3-26.7 and S=32.7-34 (Figure S2b). Two lower values of Cd_{dyn} (S=15.35 and S=17.95; sites 10 and 11) suggest that locally very active complexing agents may fix part of the Cd_{diss} in a non-dynamic form. Various hydrodynamic processes including tidal shear stress and subsequent particles remobilization (potential ligands of Cd_{dyn}) may also be involved but not visible in SPM data. These sampling sites are yet located in one of the area where sediments dredged elsewhere for navigational purposes are re-deposited (SMIDDEST, 2016). Mid-salinity maximum values of $Cd_{0.2}$ were half than those reported in the literature for high discharge conditions (Q ~ 2,400 $m^3.s^{-1}$; probably due to Cd-rich bottom sediment resuspension; Audry et al., 2007) and close to the values observed for low discharge conditions (0.1 $\mu g.L^{-1}$; Q ~ 570 $m^3.s^{-1}$; Audry et al., 2007) as occurring during our study (0.08 $\mu g.L^{-1}$; Q ~ 235 $m^3.s^{-1}$). The literature also reports that this $Cd_{0.2}$ behavior is not seasonally dependent but equally observed throughout the year.

The range of Cd_{part} obtained from the present work was similar to that reported in previous studies (Audry et al., 2007; Boutier et al., 2000; Kraepiel et al., 1997). Audry et al. (2007) reported a sharp decrease of Cd_{part} concentrations between the freshwater endmember and the saline estuary (from 4 to 0.6 $mg.kg^{-1}$) where concentrations were rather constant, varying between 0.3 and 0.7 $mg.kg^{-1}$. Our data suggested a decrease of Cd_{part} from 0.5 to 0.3 $mg.kg^{-1}$ from S=0.1 to S=1.1 which seems

to be related to lithogenic effects since the Th-normalized Cd_{part} profile is constant along the salinity gradient until S=30.45, except for a single greater value at S=4.3. This outlier is also slightly observed in Th-normalized Pb_{part} and could be associated to a local contamination in this other zone where sediment are deposited after dredging (SMIDDEST, 2016). Clear maxima were observed in the southern coastal estuary with values reaching ~ 1 $mg.kg^{-1}$ and confirmed by Th-normalized profile. Such processes might be related to Cd adsorption or uptake by primary producers (Boutier et al., 2000; Strady et al., 2011). This hypothesis is supported by the POC% data that increase towards the coastal zone.

Copper

Biotic processes may partly explain Cu_{diss} fluvial maxima, but one cannot exclude anthropogenic source of Cu_{diss}, which is especially true for the fluvial estuary in the Bordeaux conurbation and its wastewater treatment plant effluents. Previous studies performed during a low discharge period similar to this sampling campaign estimated an anthropogenic source contribution of 10 to 20 % to the observed Cu_{diss} (Petit et al., 2013). This addition of dissolved Cu occurs most likely to a non-negligible part (~ 20 %, Figure S2c) in its dynamic, i.e. potentially bioavailable form. For $Cu_{0.2}$ a sharp decrease (from 2 to 1.2 $\mu g.L^{-1}$) was then recorded from S=0.1 to S=0.2 and might be related to changes in coarse colloid interactions. Accordingly, a previous study in the riverine endmember (S < 5) performed in June 2001 reports a decreasing trend of similar amplitude for $Cu_{0.2}$ (1.5 to 0.7 $\mu g.L^{-1}$; Audry et al., 2007). This Cu_{diss} removal may be attributed to flocculation of organo-metal complexes, or colloid adsorption and/or coagulation as already reported in the Gironde Estuary (Audry et al., 2007) or in the Scheldt Estuary (Zwolsman et al., 1997). Thereafter, both $Cu_{0.2}$ and $Cu_{0.02}$ showed similar concentrations and a non-conservative (addition) behavior in the low salinity range (S=0.2 to S=4.3), followed by steady dilution with seawater as previously observed (Dabrin, 2009). Budget estimations reported in Audry et al. (2007) suggested that Cu_{diss} in the riverine endmember are higher than predicted, revealing Cu_{diss} addition in the fluvial estuary. The Cu_{diss} reported in this study were close to values measured in samples from 2001 and 2007 (Audry et al., 2007; Dabrin, 2009). Yet, the low proportion of Cu_{dyn} displayed interesting features with riverine endmember levels varying from 0.06 $\mu g.L^{-1}$ (S=0.1) to ~ 0.25 $\mu g.L^{-1}$ (S=0.2 and S=1.1) that may be associated with biotic processes and/or anthropogenic inputs as discussed in *Section 3.3*.

Previous studies reported the sharpest Cu_{part} decrease with values ranging from 75 $mg.kg^{-1}$ for the freshwater endmember to 30 $mg.kg^{-1}$ (Audry et al., 2007; Kraepiel et al., 1997). Particulate Cu concentrations in the riverine part, in June 2017, were roughly twice lower than levels reported in June 2001. However, Th-normalized values suggested that these variations were rather grain-size related since the decrease was no longer observed after normalization. These previous studies reported a constant Cu_{part} throughout the salinity gradient (~ 30 $mg.kg^{-1}$), while our observations showed an increasing trend from S=25 with Cu_{part}, reaching their highest values of 300 $mg.kg^{-1}$ in the southern coastal estuary. This trend was confirmed by the Th-normalized data. As the coastal waters showed the highest POC levels, these observations were attributed to an enrichment of Cu_{part} associated to marine phytoplankton sorption (Petit et al., 2013) as discussed below.

4.2. New insights from the dynamic fraction monitoring in combination with other fractions

Photo-redox processes

The analysis of the three different dissolved metal fractions, revealed changes in the dissolved Pb speciation along the salinity gradient. For low salinities (S<10), Pb_{dyn} represented less than 10 % of the dissolved fractions while in the outer estuary it encompassed ~ 80 % of the Pb_{diss} (Figure S2a), with concentrations of ~ 0.015 $\mu g.L^{-1}$ for the four southern coastal sites (Figure 3a). A small increase in Pb_{dyn} around S=10 was concomitant with lower $Pb_{0.2}$ and $Pb_{0.02}$ values and a SPM peak which may be related to sediment remobilization processes (Figure 2b and Figure 3a). Yet, another similar Pb_{dyn} increase also occurred at S=25. Previous studies on biogeochemical cycles of Pb_{diss} showed that photolysis of colloidal OM and the photo-redox cycling of colloidal metal(hydrous)oxides cause a daytime decrease of colloidal Pb (0.2 – 0.02 µm) in coastal systems (Pinedo-Gonzalez et al., 2014). A study of Pb_{diss} measured by ASV in the Krka Estuary showed that, despite an enhanced formation of electroactive Pb chloro-complexes through increasing salinity, ~ 30 to 40 % of total Pb bound to strong complexes may be degraded after solar radiation (Omanović et al., 2006). Such photo-redox processes may contribute to intra-estuarine increases of Pb_{dyn} which is supported by the significantly positive correlation of this fraction variations with rad/SPM (r = 0.614; Table S1). Tercier-Waeber et al. (2009) also observed daytime increases of Pb_{dyn} and Cd_{dyn} that were induced by photoreduction/reoxidation of colloidal metal oxides, especially small (< 0.02 µm) colloidal Mn oxides in rivers. Variations of Fe_{diss} and Mn_{diss} along the estuarine gradient do not allow one to observe Fe-Mn colloid influence on dynamic trace metal

fraction while the POC increase seawards suggests an increasing importance of organic particles as trace metal carrier phase. In the Gironde coastal waters, very low SPM (in comparison with intra-estuarine levels) may therefore favor the relatively high Pb_{dyn} with Pb-bearing organic colloids photolysis releasing dynamic Pb species. The nature of this colloidal fraction remains to be determined but may be biogenic, originating from small algal cell debris and/or phytoplankton exudates (extracellular organic polymeric matter). Monitoring of the Pb_{dyn} performed with the TracMetal supports previous assumptions by Pinedo-Gonzalez et al. (2014, and references therein) that soluble metals generated by both colloid photolysis/photoreduction processes in seawater can be significantly biologically active and play an important role enhancing trace metal availability. Stronger biological interactions (sorption processes) with Cd than with Pb (e.g. Tercier-Waeber et al., 2009) may explain the observed lower proportion of Cd_{dyn} (~ 30 % of Cd_{diss}) in the southern coastal sites compared to Pb_{dyn} (~ 60 % of Pb_{diss}).

Biotic processes

The literature reports that the distribution of Cu_{diss} along the Gironde Estuary salinity gradient displays strong seasonal variability (Audry et al., 2007). When entering the MTZ, with SPM > 1,500 $mg.L^{-1}$ (Figure 2b), in the very low salinity range, riverine phytoplankton and bacteria experience turbidity and salinity stress which cause cell lysis (Fisher et al., 1998; Goosen et al., 1999). Subsequent release of bioaccumulated/adsorbed Cu supports the notion that microbially-driven OM degradation explains Cu_{diss} addition in the turbidity gradient (Petit et al., 2013). The typical rapid drop of POC% from 2 % at S=0.1 to 1.1 % at S=1.1 (Figure 2d) has been attributed to the mineralization of the organic-rich riverine SPM (heterotrophic activity) and parallel dilution with organic-poor particles in the MTZ with this zone showing constant POC% values of ~ 1.5 % (Abril et al., 2002; Etcheber et al., 2007; Masson et al., 2011; Petit et al., 2013). These processes may cause Cu addition since this element exhibits a strong affinity to OM (> 95 % of Cu in seawater is complexed with organic ligands; Sunda and Huntsman, 1991). Our study showed an increasing trend in POC% levels along the salinity gradient from 2 % at S>6 to 15 % at S=31.85. Assuming that in the low turbidity, high salinity range near the estuary mouth, POC is a proxy for algal cell presence, biological sorption by phytoplankton during the bloom period might therefore also contribute to continuous Cu_{diss} removal, which is supported by the continuous Cu_{part} and P_{Cu} increase along the gradient observed in our study (Figures 3f and S2d). Significant negative

correlations were observed between rad/SPM and $Cu_{0.2}$ as well as $Cu_{0.02}$ ($r = 0.740$ and 0.663, respectively. Table S1) suggesting the increasing phytoplankton sorption of dissolved Cu with increasing effective radiation along the estuary. Previous studies report ~ 50 % removal of Cu_{diss} in the Atlantic Ocean surface waters due to biological activity during spring (Kremling and Pohl, 1989). Pearson r correlation between Me_{part} and POC% were of -0.1 for Pb, 0.4 for Cd, and 0.7 for Cu, while a typical lithogenic trace element such as Th gave a correlation of -0.9 (data not shown). Such values support the increasing biotic removal (subtraction) of dissolved Cu through cell sorption together with increasing phytoplankton load, especially in the outer estuary where algal accumulation likely represents a seasonal net sink of Cu, and Cd (Audry et al., 2007; Boutier et al., 2000; Dabrin et al., 2014; Strady et al., 2011).

Ecotoxicological implications

For all trace metals, various biogeochemical processes that lead to Me_{dyn} release may be of concern for wild living organisms. In the outer estuary, the dynamic fraction represents only 40-50% of Cd_{diss} (Figure S2b). A lower proportion of Cd_{dyn} (compared to intra-estuarine sites) suggests the importance of small colloids in distribution of Cd in the outer estuary with stronger complexation by marine OM (algae as supported by POC%) that may transform dynamic Cd into non-dynamic forms. The dominance of Cd_{dyn} fraction along the salinity gradient followed by important Cd_{dyn} complexation by algal cells in the estuary mouth is of major ecotoxicological concern. Indeed, historical Cd contamination of the Gironde Estuary has resulted in oyster farming being prohibited in this system, while the Marennes-Oléron Bay, located further north, hosts the largest oyster production in France and even Europe (Michel et al., 2000; Strady et al., 2011). Because the Marennes-Oléron Bay is influenced by the polymetallic (especially Cd) pollution of the Gironde Estuary (e.g. Boutier et al., 2000; Strady et al., 2011), the understanding of Cd dynamics, speciation and associated oyster contamination is crucial. This contamination may occur from the likely dominant direct pathway i.e. from the dissolved phase (e.g. Lekhi et al., 2008), or through the trophic pathway (phytoplankton consumption and/or ingested fine particles e.g. Ramteke et al., 2021). In the Gironde system, Cd bioaccumulation by oysters most likely occurs through both contamination pathways (Strady et al., 2011), yet this element has a strong affinity for the dissolved phase, (relatively low P_{Cd} values compared to the other studied metals; Figure S1c; Chiffoleau et al., 1994; Kraepiel et al., 1997). Therefore, considering the dominance of Cd_{dyn} along the gradient,

potential algal sorption in the coastal waters observed in this study may reduce the availability of Cd to marine oysters (through uptake from the dissolved phase). The seasonality of algal blooms may influence the availability of Cd_{dyn} to filter feeders and requires further study under different seasonal and hydrological conditions. The TracMetal is therefore an efficient sensing and sentinel tool for freshly mobilized, dynamic metal species to observe processes that are only partly visible or not monitored with only conventional dissolved fractions.

Overall, contamination levels recorded for trace metals in this study were at least twice lower than ~ 20 years ago (Audry et al., 2007; Kraepiel et al., 1997). Estuarine dissolved Cd fluxes exported to the ocean were shown to be eight times lower than ~ 40 years ago and imply a general decrease of Cd pollution in Gironde wild oysters (Lanceleur et al., 2011; Pougnet et al., 2021). These observations may be related to the decreased anthropogenic trace metal emissions in this region combined with the modification of the hydrodynamic regime of the system with, in particular, a decreasing trend in river discharge (Boyle et al., 2014; Jalón-Rojas et al., 2015; Pougnet et al., 2021).

5. Conclusions and Perspectives

The speciation and partitioning of trace metals in the Gironde Estuary has been studied for decades but this study completes its understanding by performing the first assessment of the dynamic fraction of the trace elements related to key biogeochemical processes. In the riverine branch, biogeochemical reactivity of Cu (release by OM mineralization in the MTZ; Petit et al., 2013) may explain the important proportion of the dynamic fraction in the dissolved phase. For Cd, the dynamic fraction may represent up to 90% of the dissolved phase along the salinity gradient. This observation is of major concern considering the potential bioavailability of trace metal dynamic fractions. The dissolved phase < 0.02 µm is conventionally referred to as the "truly" dissolved fractions. This is the most bioavailable fraction containing the free metal ions and therefore the potentially the most toxic (e.g. Masson et al., 2011). Monitoring of the TracMetal in the Gironde Estuary has shown that Cu_{dyn} represented only a minor fraction of dissolved Cu < 0.02 µm, which points to the importance of small colloids in estuarine dissolved Cu speciation. Similar observations were recently reported for arsenic (As) in the same system (Penezić et al., 2020) highlighting the need to reconsider the "truly" dissolved fraction from an ecotoxicological point of view. The application of the TracMetal also shed light on photo-redox processes by detecting an increasing dynamic species concentration especially for Pb_{dyn} along the estuary and near the Gironde Estuary mouth. This is where low SPM and intense light penetration occurred in the water column, probably impacting biogenic colloids. In coastal waters, phytoplankton influences the distribution of trace metals and may act as efficient scavenger to trap trace metals in the particulate phase, possibly explaining the decrease in the proportion of the Cd_{dyn} fraction coupled to the increase of Cd_{part}. All these new finding support the need for a closer monitoring of processes occurring in productive coastal zones. Considering the wide range of potential metal carrying phases, the application of the TracMetal state-of-the-art monitoring device at high temporal and spatial scales allows one to observe and interpret biogeochemical processes that are not accessible by conventional methods. Bioavailability-oriented methods should therefore be considered in ecotoxicological risk assessment of metals and regulations (Merrington et al., 2017; Verweij et al., 1992).

Acknowledgements

This work has benefited from financial supports by the EU FP7 Ocean 2013.2 Project SCHeMA (Project-Grant Agreement 614002), the Regional Water Agency (Agence de l'Eau Adour-Garonne) the FEDER Aquitaine-1999-Z0061, and the Portuguese FCT (M. Abdou contract, CEECIND/01777/2018), which are gratefully acknowledged. Authors also gratefully acknowledge the help of the R/V Thalia Crew (TGIR FOF); Dr. A. Penezić, Dr. T. Gil-Díaz, Dr. C. Catrouillet, Dr. A. Lerat, L. Troi, Dr. C. Charbonnier, D. Poirier, A. Charrier, and C. Pereto, for sampling and assistance during field campaigns, ancillary parameter analyses, as well as scientific support; Dr. K. Fauquembergue and Dr. P. Maroni for support in data presentation.

References

Abril, G., Nogueira, M., Etcheber, H., Cabeçadas, G., Lemaire, E., Brogueira, M.J., 2002. Behaviour of Organic Carbon in Nine Contrasting European Estuaries. Estuarine Coastal and Shelf Science 54, 241–262. https://doi.org/10.1006/ecss.2001.0844

Audry, S., Blanc, G., Schäfer, J., Guérin, F., Masson, M., Robert, S., 2007. Budgets of Mn, Cd and Cu in the macrotidal Gironde estuary (SW France). Marine Chemistry 107, 433–448. https://doi.org/10.1016/j.marchem.2007.09.008

Audry, S., Schäfer, J., Blanc, G., Jouanneau, J.-M., 2004. Fifty-year sedimentary record of heavy metal pollution (Cd, Zn, Cu, Pb) in the Lot River reservoirs (France). Environmental Pollution 132, 413–426. https://doi.org/10.1016/j.envpol.2004.05.025

Bourg, A.C.M., 1987. Trace metal adsorption modelling and particle-water interactions in estuarine environments. Continental Shelf Research 7, 1319–1332. https://doi.org/10.1016/0278-4343(87)90036-7

Boutier, B., Chiffoleau, J.-F., Gonzalez, J.-L., Lazure, P., Auger, D., Truquet, I., 2000. Influence of the Gironde estuary outputs on cadmium concentrations in the waters: consequences on the Marennes-Oléron bay (France). Oceanologica Acta 23, 745–757. https://doi.org/10.1016/S0399-1784(00)01119-1

Boyle, E., Lee, J.-M., Echegoyen, Y., Noble, A., Moos, S., Carrasco, G., Zhao, N., Kayser, R., Zhang, J., Gamo, T., Obata, H., Norisuye, K., 2014. Anthropogenic Lead Emissions in the Ocean: The Evolving Global Experiment. oceanog 27, 69–75. https://doi.org/10.5670/oceanog.2014.10

Braungardt, C.B., Achterberg, E.P., Axelsson, B., Buffle, J., Graziottin, F., Howell, K.A., Illuminati, S., Scarponi, G., Tappin, A.D., Tercier-Waeber, M.-L., Turner, D., 2009. Analysis of dissolved metal fractions in coastal waters: An inter-comparison of five voltammetric in situ profiling (VIP) systems. Marine Chemistry 114, 47–55. https://doi.org/10.1016/j.marchem.2009.03.006

Buffle, J., Tercier-Waeber, M.-L., 2005. Voltammetric environmental trace-metal analysis and speciation: from laboratory to in situ measurements. TrAC Trends in Analytical Chemistry, Trace-metal analysis 24, 172–191. https://doi.org/10.1016/j.trac.2004.11.013

Castelle, S., Schäfer, J., Blanc, G., Dabrin, A., Lanceleur, L., Masson, M., 2009. Gaseous mercury at the air–water interface of a highly turbid estuary (Gironde Estuary, France). Marine Chemistry, 10th International Estuarine Biogeochemistry Symposium - "Estuaries in a Changing World" 117, 42–51. https://doi.org/10.1016/j.marchem.2009.01.005

Chiffoleau, J.-F., Cossa, D., Auger, D., Truquet, I., 1994. Trace metal distribution, partition and fluxes in the Seine estuary (France) in low discharge regime. Marine Chemistry 47, 145–158. https://doi.org/10.1016/0304-4203(94)90105-8

Coynel, A., Blanc, G., Marache, A., Schäfer, J., Dabrin, A., Maneux, E., Bossy, C., Masson, M., Lavaux, G., 2009. Assessment of metal contamination in a small mining- and smelting-affected watershed: high resolution monitoring coupled with spatial analysis by GIS. J. Environ. Monit. 11, 962–976. https://doi.org/10.1039/B818671E

Dabrin, A., 2009. Mécanismes de transfert des éléments traces métalliques (ETM) et réactivité estuarienne : cas des systèmes Gironde, Charente, Seudre et Baie de Marennes Oléron (These de doctorat). Bordeaux 1.

Dabrin, A., Schäfer, J., Bertrand, O., Masson, M., Blanc, G., 2014. Origin of suspended matter and sediment inferred from the residual metal fraction: Application to the Marennes Oleron

Bay, France. Continental Shelf Research 72, 119–130. https://doi.org/10.1016/j.csr.2013.07.008
Dabrin, A., Schäfer, J., Blanc, G., Strady, E., Masson, M., Bossy, C., Castelle, S., Girardot, N., Coynel, A., 2009. Improving estuarine net flux estimates for dissolved cadmium export at the annual timescale: Application to the Gironde Estuary. Estuarine, Coastal and Shelf Science 84, 429–439. https://doi.org/10.1016/j.ecss.2009.07.006
Deycard, V.N., Schäfer, J., Blanc, G., Coynel, A., Petit, J.C.J., Lanceleur, L., Dutruch, L., Bossy, C., Ventura, A., 2014. Contributions and potential impacts of seven priority substances (As, Cd, Cu, Cr, Ni, Pb, and Zn) to a major European Estuary (Gironde Estuary, France) from urban wastewater. Marine Chemistry, Estuarine Biogeochemistry 167, 123–134. https://doi.org/10.1016/j.marchem.2014.05.005
Deycard, V.N., Schäfer, J., Petit, J.C.J., Coynel, A., Lanceleur, L., Dutruch, L., Bossy, C., Ventura, A., Blanc, G., 2017. Inputs, dynamics and potential impacts of silver (Ag) from urban wastewater to a highly turbid estuary (SW France). Chemosphere 167, 501–511. https://doi.org/10.1016/j.chemosphere.2016.09.154
Dutruch, L., Schäfer, J., Abdou, M., Kutscher, D., 2019. Direct analysis of trace elements in estuarine waters using triple-quadrupole inductively coupled plasma- mass spectrometry 15, 4.
Elbaz-Poulichet, F., Holliger, P., Wen Huang, W., Martin, J.-M., 1984. Lead cycling in estuaries, illustrated by the Gironde estuary, France. Nature 308, 409–414. https://doi.org/10.1038/308409a0
Etcheber, H., Taillez, A., Abril, G., Garnier, J., Servais, P., Moatar, F., Commarieu, M.-V., 2007. Particulate organic carbon in the estuarine turbidity maxima of the Gironde, Loire and Seine estuaries: origin and lability. Hydrobiologia 588, 245–259. https://doi.org/10.1007/s10750-007-0667-9
Fighera, M., Wal, P.D.V. der, Tercier-Waeber, M.-L., Shea, H., 2016. Three-Electrode on-Chip Sensors for Voltammetric Detection of Trace Metals in Natural Waters. ECS Trans. 75, 303. https://doi.org/10.1149/07516.0303ecst
Fisher, T.R., Hagy, J.D., Rochelle-Newall, E., 1998. Dissolved and particulate organic carbon in Chesapeake Bay. Estuaries 21, 215–229. https://doi.org/10.2307/1352470
Gil-Díaz, T., Schäfer, J., Coynel, A., Bossy, C., Dutruch, L., Blanc, G., Gil-Díaz, T., Schäfer, J., Coynel, A., Bossy, C., Dutruch, L., Blanc, G., 2018. Antimony in the Lot–Garonne river system: a 14-year record of solid–liquid partitioning and fluxes. Environ. Chem. 15, 121–136. https://doi.org/10.1071/EN17188
Goosen, N.K., Kromkamp, J., Peene, J., van Rijswijk, P., van Breugel, P., 1999. Bacterial and phytoplankton production in the maximum turbidity zone of three European estuaries: the Elbe, Westerschelde and Gironde. Journal of Marine Systems 22, 151–171. https://doi.org/10.1016/S0924-7963(99)00038-X
Illuminati, S., Annibaldi, A., Truzzi, C., Tercier-Waeber, M.-L., Nöel, S., Braungardt, C.B., Achterberg, E.P., Howell, K.A., Turner, D., Marini, M., Romagnoli, T., Totti, C., Confalonieri, F., Graziottin, F., Buffle, J., Scarponi, G., 2019. In-situ trace metal (Cd, Pb, Cu) speciation along the Po River plume (Northern Adriatic Sea) using submersible systems. Marine Chemistry 212, 47–63. https://doi.org/10.1016/j.marchem.2019.04.001
Jalón-Rojas, I., Schmidt, S., Sottolichio, A., 2015. Turbidity in the fluvial Gironde Estuary (southwest France) based on 10-year continuous monitoring: sensitivity to hydrological conditions. Hydrol. Earth Syst. Sci. 19, 2805–2819. https://doi.org/10.5194/hess-19-2805-2015

Jouanneau, J.M., Lapaquellerie, Y., Latouche, C., 1993. Origin and pathways of Cadmium Contamination in the Gironde estuary, Garonne river and tributaries., in: Vernet, J.-P. (Ed.), Studies in Environmental Science. Elsevier, pp. 373–389. https://doi.org/10.1016/S0166-1116(08)70302-9

Kraepiel, A.M.L., Chiffoleau, J.-F., Martin, J.-M., Morel, F.M.M., 1997. Geochemistry of trace metals in the Gironde estuary. Geochimica et Cosmochimica Acta 61, 1421–1436. https://doi.org/10.1016/S0016-7037(97)00016-1

Kremling, K., Pohl, C., 1989. Studies on the spatial and seasonal variability of dissolved cadmium, copper and nickel in northeast atlantic surface waters. Marine Chemistry 27, 43–60. https://doi.org/10.1016/0304-4203(89)90027-3

Lanceleur, L., Schäfer, J., Chiffoleau, J.-F., Blanc, G., Auger, D., Renault, S., Baudrimont, M., Audry, S., 2011. Long-term records of cadmium and silver contamination in sediments and oysters from the Gironde fluvial–estuarine continuum – Evidence of changing silver sources. Chemosphere 85, 1299–1305. https://doi.org/10.1016/j.chemosphere.2011.07.036

Larrose, A., Coynel, A., Schäfer, J., Blanc, G., Massé, L., Maneux, E., 2010. Assessing the current state of the Gironde Estuary by mapping priority contaminant distribution and risk potential in surface sediment. Applied Geochemistry 25, 1912–1923. https://doi.org/10.1016/j.apgeochem.2010.10.007

Lekhi, P., Cassis, D., Pearce, C.M., Ebell, N., Maldonado, M.T., Orians, K.J., 2008. Role of dissolved and particulate cadmium in the accumulation of cadmium in cultured oysters (Crassostrea gigas). Sci. Total Environ. 393, 309–325. https://doi.org/10.1016/j.scitotenv.2007.12.004

Lerat-Hardy, A., Coynel, A., Schäfer, J., Marache, A., Pereto, C., Bossy, C., Capdeville, M.-J., Granger, D., 2021. Impacts of Highway Runoff on Metal Contamination Including Rare Earth Elements in a Small Urban Watershed: Case Study of Bordeaux Metropole (SW France). Arch Environ Contam Toxicol. https://doi.org/10.1007/s00244-021-00816-4

Loring, D.H., Rantala, R.T.T., 1992. Manual for the geochemical analyses of marine sediments and suspended particulate matter. Earth-Science Reviews 32, 235–283. https://doi.org/10.1016/0012-8252(92)90001-A

Marmolejo-Rodríguez, A.J., Caetano, M., Prego, R., Vale, C., 2008. Thorium accumulation in the sedimentary environment of the Vigo Ria (NW Iberian Peninsula). Journal of Environmental Radioactivity, Natural Radiation 99, 1631–1635. https://doi.org/10.1016/j.jenvrad.2008.06.008

Masson, M., Blanc, G., Schäfer, J., 2006. Geochemical signals and source contributions to heavy metal (Cd, Zn, Pb, Cu) fluxes into the Gironde Estuary via its major tributaries. Science of The Total Environment 370, 133–146. https://doi.org/10.1016/j.scitotenv.2006.06.011

Masson, M., Blanc, G., Schäfer, J., Parlanti, E., Le Coustumer, P., 2011. Copper addition by organic matter degradation in the freshwater reaches of a turbid estuary. Science of The Total Environment 409, 1539–1549. https://doi.org/10.1016/j.scitotenv.2011.01.022

McKinley, I.G., Alexander, W.R., 1992. Constraints on the applicability of 'in-situ distribution coefficient' values. Journal of Environmental Radioactivity 15, 19–34. https://doi.org/10.1016/0265-931X(92)90040-Z

Merrington, G., Peters, A., Schlekat, C.E., 2017. Accounting for metal bioavailability in assessing water quality: A step change? Environmental Toxicology and Chemistry 257–265. https://doi.org/10.1002/etc.3252@10.1002/(ISSN)1552-8618.REACH

Michel, P., Boutier, B., Chiffoleau, J.-F., 2000. Net Fluxes of Dissolved Arsenic, Cadmium, Copper, Zinc, Nitrogen and Phosphorus from the Gironde Estuary (France): Seasonal

Variations and Trends. Estuarine, Coastal and Shelf Science 51, 451–462. https://doi.org/10.1006/ecss.2000.0691
Nezamzadeh-Ejhieh, A., Shahanshahi, M., 2013. Modification of clinoptilolite nano-particles with hexadecylpyridynium bromide surfactant as an active component of Cr(VI) selective electrode. Journal of Industrial and Engineering Chemistry 19, 2026–2033. https://doi.org/10.1016/j.jiec.2013.03.018
Omanović, D., Kwokal, Ž., Goodwin, A., Lawrence, A., Banks, C.E., Compton, R.G., Komorsky-Lovrić, Š., 2006. Trace metal detection in Šibenik Bay, Croatia: Cadmium, lead and copper with anodic stripping voltammetry and manganese via sonoelectrochemistry. A case study. JICS 3, 128–139. https://doi.org/10.1007/BF03245940
Penezić, A., Tercier-Waeber, M.-L., Abdou, M., Bossy, C., Dutruch, L., Bakker, E., Schäfer, J., 2020. Spatial variability of arsenic speciation in the Gironde Estuary: Emphasis on dynamic (potentially bioavailable) inorganic arsenite and arsenate fractions. Marine Chemistry 103804. https://doi.org/10.1016/j.marchem.2020.103804
Petit, J.C.J., Schäfer, J., Coynel, A., Blanc, G., Deycard, V.N., Derriennic, H., Lanceleur, L., Dutruch, L., Bossy, C., Mattielli, N., 2013. Anthropogenic sources and biogeochemical reactivity of particulate and dissolved Cu isotopes in the turbidity gradient of the Garonne River (France). Chemical Geology 359, 125–135. https://doi.org/10.1016/j.chemgeo.2013.09.019
Pinedo-Gonzalez, P., West, A.J., Rivera-Duarte, I., Sañudo-Wilhelmy, S.A., 2014. Diel Changes in Trace Metal Concentration and Distribution in Coastal Waters: Catalina Island As a Study Case. Environ. Sci. Technol. 48, 7730–7737. https://doi.org/10.1021/es5019515
Pougnet, F., Blanc, G., Mulamba-Guilhemat, E., Coynel, A., Gil-Diaz, T., Bossy, C., Strady, E., Schäfer, J., 2021. Nouveau modèle analytique pour une meilleure estimation des flux nets annuels en métaux dissous. Cas du cadmium dans l'estuaire de la Gironde. Hydroécol. Appl. 21, 47–69. https://doi.org/10.1051/hydro/2019002
Ramteke, D., Chakraborty, P., Chennuri, K., Sarkar, A., 2021. Geochemical fractionation study in combination with equilibrium based chemical speciation modelling of Cd in finer sediments provide a better description of Cd bioavailability in tropical estuarine systems. Science of The Total Environment 764, 143798. https://doi.org/10.1016/j.scitotenv.2020.143798
Sanders, J.G., Abbe, G.R., 1987. The role of suspended sediments and phytoplankton in the partitioning and transport of silver in estuaries. Continental Shelf Research, Dynamics of Turbid Coastal Environments 7, 1357–1361. https://doi.org/10.1016/0278-4343(87)90040-9
Schäfer, J., Blanc, G., 2002. Relationship between ore deposits in river catchments and geochemistry of suspended particulate matter from six rivers in southwest France. Science of The Total Environment 298, 103–118. https://doi.org/10.1016/S0048-9697(02)00196-1
Schäfer, J., Blanc, G., Lapaquellerie, Y., Maillet, N., Maneux, E., Etcheber, H., 2002. Ten-year observation of the Gironde tributary fluvial system: fluxes of suspended matter, particulate organic carbon and cadmium. Marine Chemistry, 6th International Symposium on Model Estuaries 79, 229–242. https://doi.org/10.1016/S0304-4203(02)00066-X
Schäfer, J., Coynel, A., Blanc, G., 2021. Impact of metallurgy tailings in a major European fluvial-estuarine system: Trajectories and resilience over seven decades. Sci Total Environ 805, 150195. https://doi.org/10.1016/j.scitotenv.2021.150195
Seijo, M., Ulrich, S., Filella, M., Buffle, J., Stoll, S., 2009. Modeling the Adsorption and Coagulation of Fulvic Acids on Colloids by Brownian Dynamics Simulations. Environ. Sci. Technol. 43, 7265–7269. https://doi.org/10.1021/es9002394

Shiller, A., Boyle, E., 1991. Trace Elements in the Mississippi River Delta Outflow Region: Behavior at High Discharge. Geochimica et Cosmochimica Acta 55, 3241–3251.
SMIDDEST, 2016. Elaboration du plan de gestion des sediments de dragage de l'estuaire de la Gironde 51.
Strady, E., Blanc, G., Baudrimont, M., Schäfer, J., Robert, S., Lafon, V., 2011. Roles of regional hydrodynamic and trophic contamination in cadmium bioaccumulation by Pacific oysters in the Marennes-Oléron Bay (France). Chemosphere 84, 80–90. https://doi.org/10.1016/j.chemosphere.2011.02.051
Sunda, W.G., 1989. Trace Metal Interactions with Marine Phytoplankton. Biological Oceanography 6, 411–442. https://doi.org/10.1080/01965581.1988.10749543
Sunda, W.G., Huntsman, S.A., 1991. The use of chemiluminescence and ligand competition with EDTA to measure copper concentration and speciation in seawater. Marine Chemistry, Reactivity of Chemical Species in Aquatic Environments 36, 137–163. https://doi.org/10.1016/S0304-4203(09)90059-7
Tercier Waeber, M.-L., Bakker, E., Nardin, C., Mongin, S., Prado, E., Cuartero Botia, M., Mazaikoff, B., Luxenburger, F., Klimant, I., Mistlberger, G., Mueller, B., Van Der Val, P., Fighera, M., Fernandez Sanchez, J., Medina Castillo, A.L., Navarro, A.V., Schaefer, J., Abdou, M., Novellino, A., D'Angelo, P., Confalonieri, F., Castellano, M., Magi, E., Massa, F., Povero, P., 2015. FP7-OCEAN-2013 — SCHeMA: Integrated in situ chemical mapping probes, in: OCEANS 2015 - Genova. Presented at the OCEANS 2015 - Genova, pp. 1–5. https://doi.org/10.1109/OCEANS-Genova.2015.7271560
Tercier Waeber, M.-L., Buffle, J., Graziottin, F., 1998. A Novel Voltammetric In-Situ Profiling System for ContinuousReal-Time Monitoring of Trace Elements in Natural Waters. Electroanalysis 10, 355–363. https://doi.org/10.1002/(SICI)1521-4109(199805)10:6<355::AID-ELAN355>3.0.CO;2-F
Tercier Waeber, M.-L., Stoll, S., Slaveykova, V., 2012. Trace metal behavior in surface waters: emphasis on dynamic speciation, sorption processes and bioavailability. Archives des Sciences 65, 119–142.
Tercier-Waeber, M.-L., Abdou, M., Fighera, M., Kowal, J., Bakker, E., van der Wal, P., 2021a. In Situ Voltammetric Sensor of Potentially Bioavailable Inorganic Mercury in Marine Aquatic Systems Based on Gel-Integrated Nanostructured Gold-Based Microelectrode Arrays. ACS Sens. https://doi.org/10.1021/acssensors.0c02111
Tercier-Waeber, M.-L., Buffle, J., Confalonieri, F., Riccardi, G., Sina, A., Graziottin, F., Fiaccabrino, G.C., Koudelka-Hep, M., 1999. Submersible voltammetric probes for in situ real-time trace element measurements in surface water, groundwater and sediment-water interface. Meas. Sci. Technol. 10, 1202–1213. https://doi.org/10.1088/0957-0233/10/12/312
Tercier-Waeber, M.-L., Confalonieri, F., Abdou, M., Dutruch, L., Bossy, C., Fighera, M., Bakker, E., Graziottin, F., van der Wal, P., Schäfer, J., 2021b. Advanced multichannel submersible probe for autonomous high-resolution in situ monitoring of the cycling of the potentially bioavailable fraction of a range of trace metals. Chemosphere 131014. https://doi.org/10.1016/j.chemosphere.2021.131014
Tercier-Waeber, M.-L., Hezard, T., Masson, M., Schäfer, J., 2009. In Situ Monitoring of the Diurnal Cycling of Dynamic Metal Species in a Stream under Contrasting Photobenthic Biofilm Activity and Hydrological Conditions. Environ. Sci. Technol. 43, 7237–7244. https://doi.org/10.1021/es900247y

804 Verweij, W., Glazewski, R., Haan, H.D., 1992. Speciation of copper in relation to its
805 bioavailability. Chemical Speciation & Bioavailability 4, 43–51.
806 https://doi.org/10.1080/09542299.1992.11083177
807 Waeles, M., Riso, R.D., Le Corre, P., 2005. Seasonal variations of cadmium speciation in the Penzé
808 estuary, NW France. Estuarine, Coastal and Shelf Science 65, 143–152.
809 https://doi.org/10.1016/j.ecss.2005.06.002
810 Zwolsman, J.J.G., Van Eck, B.T.M., Van Der Weijden, C.H., 1997. Geochemistry of dissolved
811 trace metals (cadmium, copper, zinc) in the Scheldt estuary, southwestern Netherlands:
812 Impact of seasonal variability. Geochimica et Cosmochimica Acta 61, 1635–1652.
813 https://doi.org/10.1016/S0016-7037(97)00029-X
814